Liquid Flow in Heterogeneous Biofilms

Dirk de Beer, Paul Stoodley, and Zbigniew Lewandowski*
Center for Biofilm Engineering, 409 Cbleigh Hall, Montana State University, Bozeman, MT 59717-0398

Received January 3, 1994/Accepted April 14, 1994

Liquid flow was studied in aerobic biofilms, consisting of microbial cell clusters (discrete aggregates of densely packed cells) and interstitial voids. Fluorescein microinjection was used as a qualitative technique to determine the presence of flow in cell clusters and voids. Flow velocity profiles were determined by tracking fluorescent latex spheres using confocal microscopy. Liquid was flowing through the voids and was stagnant in the cell clusters. Consequently, in voids both diffusion and convection may contribute to mass transfer, whereas in cell clusters diffusion is the dominant factor. The flow velocity in the biofilm depended on the average flow velocity of the bulk liquid. The velocity profiles in biofilms were linear and the velocity was zero at the substratum surface. The velocity gradients within biofilms were 50% of that near walls without biofilm coverage. The influence of the biofilm roughness on the flow velocity profiles was similar to that caused by rigid roughness elements.
Key words: biofilm • hydrodynamics • mass transport • particle tracking

INTRODUCTION

Under physiological conditions almost all water-immersed surfaces are rapidly covered by biofilms, i.e., consortia of microorganisms embedded in a matrix of extracellular polymers. This may cause a variety of problems, such as increased friction resistance in pipelines and reduced heat transfer in heat exchangers.[1,3,4] Near-wall hydrodynamics determine the shear stress and the heat and mass transfer rate from the bulk liquid to the biofilm. Recently, it was found that an aerobic biofilm is constructed of cell clusters and interstitial voids.[6] Such a porous structure may enable liquid movement in the biofilm, increasing the mass transfer rate from the bulk liquid. Indirect evidence for liquid flow in biofilms on deep sea floor has been reported.[9] The effective diffusivity appeared to depend on the hydraulic regime, indicating convective mass transport in the biofilm.[17]

The hydrodynamics in smooth and rough pipes is well known for laminar and turbulent flow.[12] Because biofilms have an irregular surface,[6,7,18] they increase the wall roughness and, consequently, may increase the wall shear stress.[2–4,14] This increase in the shear stress has been attributed to increased wall roughness and to the viscoelastic properties of the biofilm,[2,4,14] due to dissipation of kinetic energy. The hydrodynamics near walls covered with biofilm has not been investigated intensively. Theoretical and experimental studies have been limited to rough surfaces, with glass beads, sand, or gravel as roughness elements,[1,8,13,19] and sediments.[5] Some of these studies conclude that the surface roughness does influence hydrodynamics if the roughness elements are larger than the thickness of the hydrodynamic boundary layer. The studies on flow near rough walls were focused on phenomena in the conduits and the upper regions of the roughness elements, below which the liquid velocity was considered zero. A virtual channel boundary was defined by extrapolating of the velocity profile in the boundary layer to zero. This approach is acceptable for calculations of wall shear stress; however, it is clearly not sufficient to understand mass transfer phenomena in biofilms, because it disregards a priori the possible intrabiofilm flow. The aim of this research was to quantify and locate liquid flow within biofilms. For that purpose, a noninvasive technique for microscale measurement, using confocal laser microscopy, of velocity profiles near and within biofilms, was developed.

MATERIALS AND METHODS

Biofilm Reactor

The reactor system, consisting of a flow cell attached to a recycle loop, has been described previously.[6] The flow cell was a rectangular polycarbonate channel with a 0.5 × 1.0 cm cross-section. A glass coverslip, serving as an observation window, was placed 15 cm from the inlet port. The flow cell, connected to the support system with flexible tubing, could be mounted on the confocal laser microscope stage. The biofilm developed on the coverslip could be microscopically examined in situ and was accessible for microcapillaries. The reactor was sterilized with a 5% NaOCl solution for 16 h and then rinsed with sterile 50 m*M* $Na_2S_2O_3$ solution to neutralize the residual chlorine. For start-up, the reactor was filled with medium[6] and inoculated with a mixture of frozen stock cultures of *Klebsiella pneumoniae*, *Pseudomonas fluorescens*, and *Pseudomonas aeruginosa*. The three species were isolated from a mature, undefined biofilm. During the initial 6 h the reactor was operated in batch mode to allow colonization of the coverslip. Subsequently, the reactor was switched to continuous culture with a liquid residence time of 26 min.

Microbiological Biofilm Analysis

At the end of the experiments an area of 1.125 cm^2 of biofilm was removed from the glass slides by scraping in

* To whom all correspondence should be addressed.

CCC 0006-3592/94/050636-06

200 mL sterile Dulbecco's phosphate buffered saline (DPBS, Sigma). Cells were dispersed by homogenization for 1 min in a Tekmar tissuemizer. Dilution series of the suspension were made with DPBS and 0.1 mL of each dilution was plated in triplicate on m-T7 agar.[10] Differentiation between colonies of the three species was based on: (1) acid production as observed from local decolorization of the agar (*Klebsiella pneumoniae*); (2) color (*Klebsiella pneumoniae* colonies are yellow, *Pseudomonas* opaque white); (3) size (*Pseudomonas aeruginosa* colonies are two to three times larger than those of *Pseudomonas fluorescens*); and (4) fluorescence (*Pseudomonas fluorescens*). From plate-count data, the amount of each species present in the biofilm was calculated and expressed as colony-forming units (CFU) per square centimeter.

Flow Velocity Measurements

Experiments were performed on 150 to 200-μm thick biofilms, developed after 4 to 5 days of growth. The structure of biofilms was visualized using confocal microscopy (Bio-Rad MRC600 in conjunction with an Olympus BH2 light microscope, 20× objective); the details of this arrangement were described previously.[6] However, instead of using fluorescent stains, which interfere with velocity measurements, biofilms were visualized using their autofluorescent properties.

The occurrence of liquid flow in cell clusters and voids was determined by local injections of small volumes of fluorescein. A nanoliter pump (Oriel A1400), supplied with a micropipette with a tip diameter of 5 to 10 μm, was used to deliver 0.16 nL fluorescein (3 m*M*) at a defined position. The pump head with micropipette was mounted on a micromanipulator with a stepper motor to enable positioning with an accuracy of 1 μm. The micropipette was prepared by pulling a 1.2-mm glass capillary to a fine tip using a heating coil. Subsequently, the capillary was softened locally and bent to a 90° angle, first at 4 mm and then at 45 mm from the tip. The resulting "J" shape allowed positioning of the microtips in the biofilm on the coverslip, by manipulating the capillary through an opening in the cover of the flow cell, downstream of the observation window. The plume, developing after the injection, was observed with confocal microscopy. In stagnant medium, the plume shape was spherical and in flowing medium was elongated. This technique was used to determine qualitatively whether the liquid was stagnant or flowing.

Local liquid velocities in the flow cell were determined by tracking the velocity of suspended fluorescent beads with confocal microscopy. Beads with a diameter of 0.3 μm (Molecular Probes, Eugene OR, ex 580), 1 μm (Polyscience, ex 458), or 24 μm (Polyscience, ex 458), having a density of 1.055 kg/L, were added to the reactor at a final concentration of 1×10^7 particles/mL. The choice of the bead diameter was determined by the desired observation distance from the coverslip, which increases with bead size. For measurements inside biofilms the small bead size was used. Particles moving slowly through the biofilm were tracked by capturing sequences of images. Velocities were calculated from the distances traveled, measured using the system software and the time elapsed between the images captured. At higher velocities, the beads appear as streaks on the screen and velocity was determined from the streak length and the scan speed. With this method only the horizontal component of the velocity was determined. Velocities were measured in a 20-μm-thick focal plane.

Hydrodynamic Calculations

The shear stress (τ) at the biofilm surface and the substratum surface was calculated from the measured velocity profiles using:

$$\tau = -\eta \frac{du}{dx} \tag{1}$$

where η is the viscosity and du/dx the velocity gradient. The shear stress for laminar flow in tubes with smooth walls was obtained from:

$$\tau = \frac{8\eta U_{avg}}{d} \tag{2}$$

where U_{avg} is the average liquid velocity in the tube and d the tube diameter.

The velocity distribution under laminar flow was calculated from the Hagen–Poiseuille equation. A liquid flowing turbulently through a tube can be divided in three regions: the viscous sublayer adjacent to the wall; the turbulent center; and the buffer zone in between these regions. Empirical equations for each of the zones were used to calculate velocity profiles.[12]

The influence of the biofilm on the hydraulic regime was estimated from the roughness Reynolds number, Re_r.[4,16] This dimensionless number is used for evaluation of the hydrodynamics near rough and rigid surfaces. If $Re_r < 5$ the regime is considered smooth, the transition from smooth to rough occurs if $5 < Re_r < 70$ and, if $Re_r > 70$, the regime is considered fully rough. The roughness Reynolds number can be calculated using:

$$Re_r = \frac{\rho U_{avg} e}{\eta} \left(\frac{f}{8}\right)^{0.5} \tag{3}$$

where ρ is the liquid density, e is the height of the roughness elements, and f the friction factor. The height of the roughness elements was assumed to be equal to the biofilm thickness. The friction factor for walls covered with biofilms was determined from the Colebrook–White equation.[16]

RESULTS

The biofilm grown from the defined mixed inoculum consisted of cell clusters of the same species attached to the substratum and voids. After 4 to 5 days of growth, the biofilm contained 10^8 CFU/cm^2 *Klebsiella pneumoniae*, 1.5

$\times 10^8$ CFU/cm^2 *Pseudomonas fluorescens*, and 5×10^8 CFU/cm^2 *Pseudomonas aeruginosa*. The thickness of the cell clusters was 150 to 200 μm and their width was 150 to 300 μm. The void fraction was approximately 50%.

Injection of 0.16 nL of 3 m*M* fluorescein resulted in the formation of a fluorescent plume. The sequence of images showed an expansion of the plume followed by a decrease in size, due to dilution of the dye. The liquid flow influenced the shape of the fluorescent plume, which was spherical in stagnant medium and elongated in flowing medium. In voids, the plume shape was influenced by the average liquid velocity in the flow cell (Fig. 1). If the medium was stagnant a spherical plume was observed, under flow conditions the plume was elongated, its length-to-width ratio depending on the liquid velocity in the flow cell (Fig. 2). In cell clusters, the plume shape was spherical at all the flow velocities applied.

Bead movement in the flow cell with a 150 to 200-μm-thick biofilm could be recorded to a depth of approximately 400 μm with 0.3-μm beads, 1000 μm with 1-μm beads, and 6000 μm with 24-μm beads. Velocity profiles measured with and without biofilm overlapped in the center part of the channel, but were significantly different in the region near the substratum (Fig. 3). In the flow cell without biofilm, profiles were parabolic and were approximately linear in the region near the substratum, between 0 and 500 μm from the surface. In the presence of biofilm two linear regions could be distinguished, one in the biofilm and another above the biofilm surface (Fig. 4). The virtual channel boundary, which is the intersect of the extrapolated velocity profile above the biofilm with the x-axis, was found 127 (±26) μm from the substratum surface, independent of the velocity of the bulk liquid. The liquid velocities in the voids were zero at the substratum surface and 2 to 15 mm/s at the biofilm–bulk interface depending on the average liquid velocity in the flow cell (U_{avg}). No movement of the cell clusters was observed under the experimental conditions.

The values for τ at the biofilm surface and the substratum surface with and without biofilm are shown in Figure 5. The shear stress at the wall without biofilm increased linearly with U_{avg}. The shear stress at the biofilm surface increased linearly with U_{avg} below 0.1 m/s. At higher U_{avg} the shear stress increased exponentially. The shear force at the substratum surface below the biofilm increased linearly with U_{avg}.

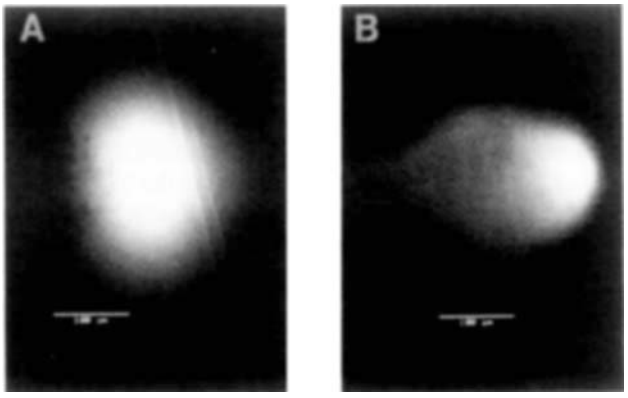

Figure 1. Confocal image of the fluorescent plume at maximal expansion in a void; U_{avg} was (A) 0 m/s and (B) 0.023 m/s.

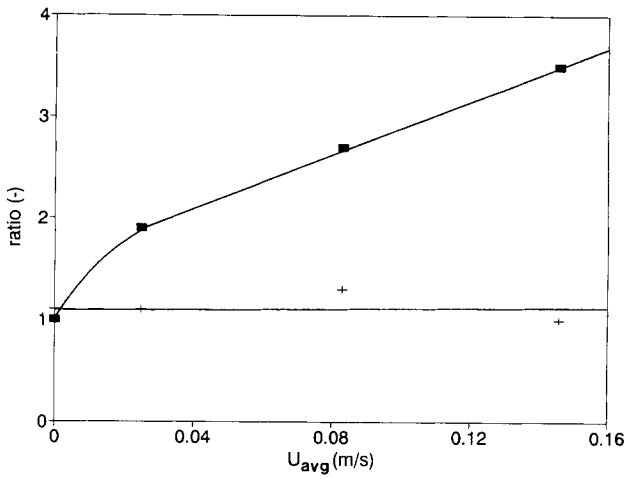

Figure 2. Ratio of the length and width of fluorescent plumes at maximal expansion in voids (■) and cell clusters (+) at various average bulk liquid velocities.

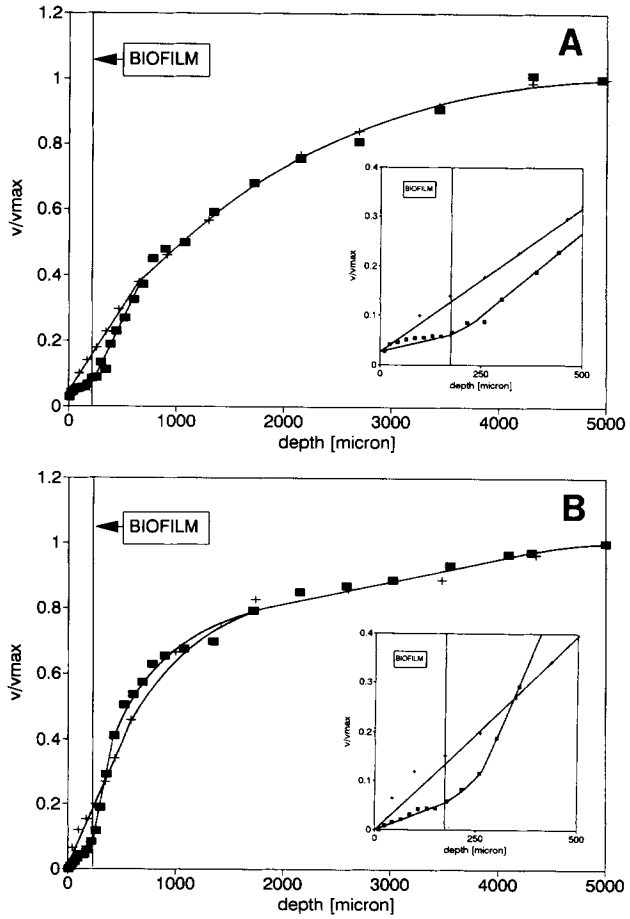

Figure 3. Normalized velocity profiles in a flow cell with (■) and without (+) biofilm; U_{avg} was (A) 0.034 m/s and (B) 0.14 m/s. The inserts are magnifications of the profiles near the substratum.

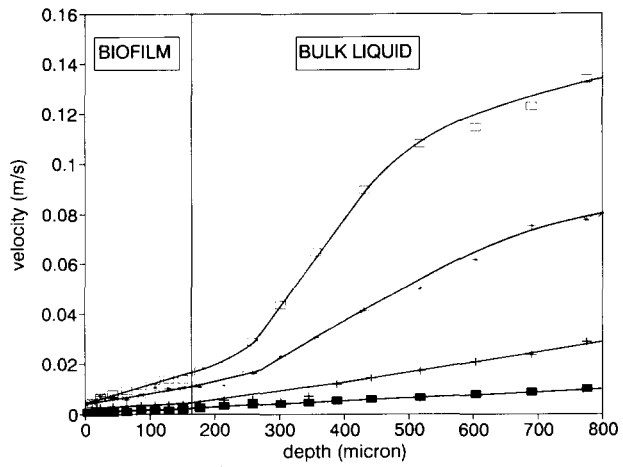

Figure 4. Velocity profiles in a flow cell with biofilm. U_{avg} was (■) 0.011 m/s, (+) 0.034 m/s, (*) 0.102 m/s, and (□) 0.165 m/s.

DISCUSSION

Although the defined community biofilm used in this study had a slightly different structure than the one of an undefined community,[6] its main characteristics were the same. The cell clusters were closely associated with the substratum and the conduits between the cell clusters and the substratum were less pronounced than in the undefined community biofilm. Therefore, liquid flow did not occur under the cell clusters.

The shape of the fluorescein plumes in the voids was spherical when the flow cell medium was stagnant and became elongated as U_{avg} was increased. In clusters the plume shape was spherical, regardless of U_{avg}, in the range of 0.008 to 0.165 m/s. This indicates that no liquid movement occurs in the cell clusters and liquid movement is possible in the voids of a biofilm. It was concluded that, in cell clusters, diffusion is the only mechanism for mass transport, whereas, in voids, both diffusion and convection may take place.

Confocal microscopy in combination with fluorescent beads enables determination of liquid velocity profiles with high spatial resolution, together with visualization of the biofilm structure. The measurements showed that the liquid movement in the voids depended on the bulk liquid velocity. The velocities at the biofilm–bulk liquid interface ranged from 0.002 to 0.015 m/s. Because the void diameter (d_v) was approximately 100 μm, *Re* in the voids ($\rho u d_v/\eta$) was lower than 1.5, indicating laminar flow.

The virtual channel boundary, the intercept of the *x*-axis and the linear extrapolation of the velocity profile in the region adjacent to the biofilm, was positioned approximately 50 μm below the top of the biofilm. It has been hypothesized that a biofilm covers a rigid wall with a viscoelastic layer, influencing the hydraulic regime in an unpredictable way.[3,4] However, microscopic observations showed no movement of the solid parts of the biofilm and the biofilm thickness was not influenced by the liquid velocity under the range of experimental conditions. In addition, the virtual channel boundary was not influenced by the liquid velocity. Consequently, the biofilms used in this study can be considered rigid in the range of experimental conditions.

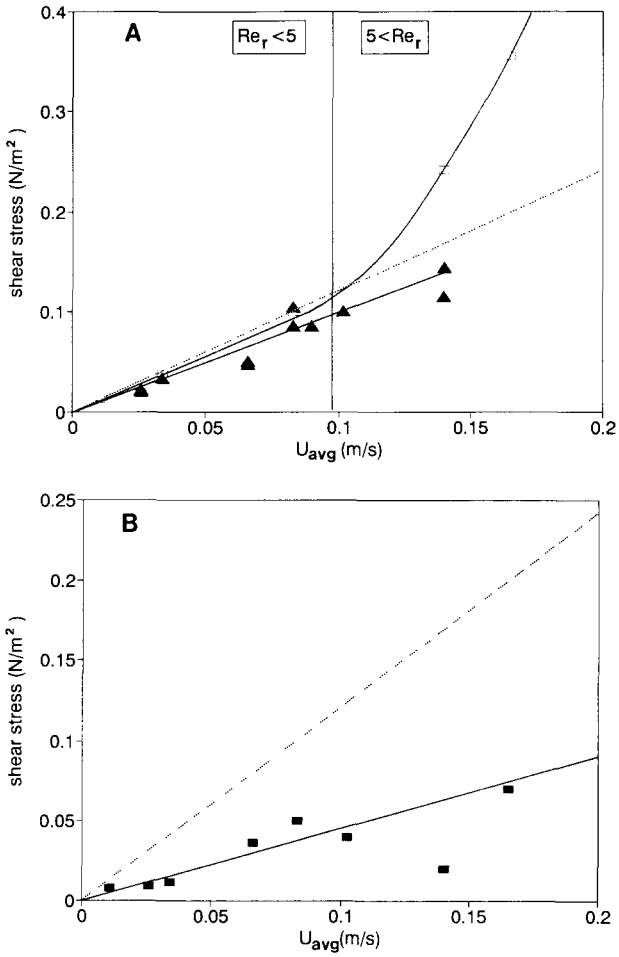

Figure 5. (A) Shear stress calculated from velocity profiles measured in a flow cell without biofilm (▲), and at the biofilm surface (□). (B) Shear stress in a flow cell with biofilm, at the substratum surface. The theoretical shear stress for laminar flow is shown as dotted line.

The roughness Reynolds number, Re_r, of the biofilm was lower than 5 for $U_{avg} < 0.1$ m/s. Consequently, under these conditions, the flow regime in the flow cell should not be influenced by the presence of the biofilm. Indeed, it was observed that the shear stress at the biofilm surface, calculated from the measured velocity gradients using Eq. (1), was close to that of a smooth surface if $U_{avg} < 0.1$ m/s. The shear stress was linearly related to the liquid velocity, similar to the theoretical relationship for laminar flow [Eq. (2)]. At higher velocities the hydraulic regime becomes gradually influenced by the presence of the biofilm and the shear stress becomes higher than predicted for smooth walls. The hydraulic conditions during the experiments were either smooth or, at the higher velocities, a transition to rough.

The velocity profiles in the viscous sublayer of the flow cell without biofilm were approximately linear. Biofilms covering the surface exert a resistance to flow, resulting in a division of velocity profile in the viscous sublayer into

two linear sections, one within and the other above the biofilm. For all measured profiles, the R^2 of both sections were above 0.9 and most were above 0.99. The ratio of the velocity gradients in the two sections was on average 0.47, if U_{avg} was lower than 0.1. At higher velocities the gradient above the biofilm increased faster than in the biofilm and, consequently, the ratio decreased. The ratio of the velocity gradients in the biofilm and those near the wall without biofilm was 0.5, in the experimental velocity range. Because the velocity at the glass surface was zero, it can be concluded that the presence of biofilm reduces the local liquid velocity by half. Considering their structure and permeability for liquids, biofilms may cautiously be compared with porous media. According to the Kozeny–Carman equation[12] the liquid velocity through a porous medium is proportional to $\epsilon^3/(1-\epsilon)^2$, ϵ being the void fraction. This relation was based on experiments for values of ϵ in the range of 0.5 to 0.6. Because ϵ was approximately 0.5, the presence of biofilm would reduce the velocity by a factor of 2, which is in agreement with our observations. Possibly, the velocity profiles in biofilms can be approximated from the void fraction and the equations for velocity distributions near smooth walls.

The difference between the velocity profiles measured with and without biofilm was only significant in the region close to the wall (Fig. 3). This was also reported previously for flow along extremely rough walls, consisting of broken glass plates and layers of spheres with a diameter of 25% of the flow cell.[15] Although, during the experiments, the Reynolds number for the flow cell ($\rho\mu d/\eta$) ranged from 50 to 1100, indicating laminar flow, the complete velocity profiles did not show perfectly laminar regimes, both in the presence and absence of biofilm. The profiles at lower velocities were closely approximated using the Hagen–Poiseuille equation, whereas, at higher velocities, the solutions for turbulent flow were more accurate (data not shown). These equations are formulated for hydraulics in smooth channels. A few theoretical studies on velocity profiles near and inside porous media have been published.[1,15] These studies describe laminar flow ($Re < 1$) over media with high porosity ($\epsilon > 0.6$) and permeability ($K > 10^{-8}$ m^2) of infinite thickness. These conditions strongly differ from those in our experiments with thin biofilms ($\epsilon = 0.5$, $K \approx 10^{-10}$ m^2). Comparison with our data showed that the models described in these other studies strongly underestimated the liquid velocities in biofilms. Consequently, they have little value for biofilm systems.

For a complete description of convective transport from the bulk liquid to the biofilm the vertical component of the flow is important, because it determines the exchange of liquid between the biofilm and the bulk. With the technique used in this study only the horizontal component of the flow can be measured. Information on the liquid exchange between biofilm and bulk liquid may be supplied by NMR measurements[11] that allow three-dimensional velocity determinations.

The observation that liquid flow occurs within a biofilm is crucial. In theoretical and experimental analyses that have been published on velocity profiles in the boundary layer above rough surfaces,[5,8,13,19] the boundary of the channel was assumed to be near the top of the rough surface, the velocity between the surface elements was assumed to be zero. Indeed, the velocity profiles measured for this study show the virtual channel boundary near the top of the biofilm. However, our measurements also show that the liquid velocity decreases gradually across the biofilm and reaches zero at the substratum surface. Further study should be directed toward modeling of velocity profiles in biofilms and the consequences of intrabiofilm flow for the mass transfer rate.

CONCLUSIONS

1. In a heterogeneous biofilm, consisting of cell clusters and voids, liquid flow is possible.
2. Liquid can flow through the voids, whereas, in the cell clusters, liquid is stagnant. Consequently, in the voids mass transport may take place by both convection and diffusion, whereas, in the cell clusters, only diffusion can occur.
3. The shear stress on the wall was increased by the presence of biofilm if $Re_r > 5$. At lower values of Re_r the biofilm had no influence on the shear stress. This is similar to the influence of rigid roughness elements on hydrodynamics.

References

1. Beavers, G. S., Joseph, D. D. 1967. Boundary conditions at a naturally permeable wall. J. Fluid Mech. **30**: 197–207.
2. Characklis, W. G. 1973. Attached microbial growth—II. Frictional resistance due to microbial slimes. Wat. Res. **7**: 1249–1258.
3. Characklis, W. G. 1981. Fouling biofilm development: a process analysis. Biotechnol. Bioeng. **13**: 1923–1960.
4. Characklis, W. G., Marshall, K. C. 1990. Biofilms. Wiley, New York.
5. Dade, W. B. 1993. Near-bed turbulence and hydrodynamic control of diffusional mass transfer at the sea floor. Limnol. Oceanogr. **38**: 52–69.
6. de Beer, D., Stoodley, P., Roe, F., Lewandowski, Z. Effects of biofilm structures on oxygen distribution and mass transport. Biotechnol. Bioeng. (in press).
7. Drury, W. J., Stewart, P. S., Characklis, W. G. 1993. Transport of 1-μm latex particles in *Pseudomonas aeruginosa* biofilms. Biotechnol. Bioeng. **42**: 111–117.
8. Grass, A. J. 1971. Structural features of turbulent flow over smooth and rough surfaces. J. Fluid Mech. **50**: 233–255.
9. Gundersen, J. K., Jorgensen, B. B., Larsen, E., Jannasch, H. W. 1992. Mats of giant sulphur bacteria on deep-sea sediments due to fluctuating hydrothermal flow. Nature **360**: 454–456.
10. LeChevalier, M. W., Cameron, S. C., McFeters, G. A. 1983. New medium for improved recovery of coliform bacteria from drinking water. Appl. Environ. Microbiol. **45**: 484–492.
11. Lewandowski, Z., Altobelli, S. A., Fukushima, E. 1993. NMR and microelectrode studies of hydrodynamics and kinetics in biofilms. Biotechnol. Prog. **9**: 40–45.

12. McGabe, W. G., Smith, J. C. 1976. Unit operations of chemical engineering. 3rd edition. McGraw-Hill, New York.
13. Nikuradze, J. 1993. Strömungsgesetze in rauhen Rohren. Forschungsheft, 361.
14. Picologlou, B. F., Zelver, N., Characklis, W. G. 1980. Biofilm growth and hydraulic performance. J. Hyd. Div. ASCE **106**: 733–746.
15. Saleh, S., Thovert, J. F., Adler, P. M. 1993. Flow along porous media by partical image velocimetry. AIChE. J. **39**: 1765–1776.
16. Schlichting, H. 1968. Boundary layer theory. McGraw-Hill, New York.
17. Siegrist, H., Gujer, W. 1985. Mas transfer mechanisms in a heterotrophic biofilm. Wat. Res. **19**: 1369–1378.
18. Steward, P. S., Peyton, B. M., Drury, W. J., Murga, R. 1993. Quantitative observations of heterogeneities in *Pseudmonas aeruginosa* biofilms. Appl. Environ. Microbiol. **59**: 327–329.
19. Willis, J. C. 1985. Near-bed velocity distribution. J. Hydr. Eng. **111**: 741–753.